

# Analytic model for the efficiency droop in semiconductors with asymmetric carrier-transport properties based on drift-induced reduction of injection efficiency

Guan-Bo Lin,<sup>1</sup> David Meyaard,<sup>1</sup> Jaehee Cho,<sup>1</sup> E. Fred Schubert,<sup>1,a)</sup> Hyunwook Shim,<sup>2</sup> and Cheolsoo Sone<sup>2</sup>

<sup>1</sup>*Future Chips Constellation and Department of Electrical, Computer, and Systems Engineering, Rensselaer Polytechnic Institute, Troy, New York 12180, USA*

<sup>2</sup>*R&D Institute, Samsung LED, Suwon 443-743, Korea*

(Received 20 February 2012; accepted 2 April 2012; published online 19 April 2012)

An analytic model is developed for the droop in the efficiency-versus-current curve for light-emitting diodes (LEDs) made from semiconductors having strong asymmetry in carrier concentration and mobility. For pn-junction diodes made of such semiconductors, the high-injection condition is generalized to include mobilities. Under high-injection conditions, electron drift in the p-type layer causes a reduction in injection efficiency. The drift-induced leakage term is shown to have a 3rd and 4th power dependence on the carrier concentration in the active region; the values of the 3rd- and 4th-order coefficients are derived. The model is suited to explain experimental efficiency-versus-current curves of LEDs. © 2012 American Institute of Physics. [<http://dx.doi.org/10.1063/1.4704366>]

The Shockley theory for pn junctions, which accurately predicts the exponential relationship between current and voltage, is limited to the low-level-injection regime.<sup>1</sup> The low-level-injection condition in an n<sup>+</sup>p junction is defined as the regime in which the injected electron concentration at the edge of the p-type neutral layer,  $\Delta n_p(0)$ , is much smaller than the equilibrium hole concentration,  $p_{p0}$ , that is

$$\Delta n_p(0) \ll p_{p0}. \quad (1)$$

This condition ensures that the conductivity of the depletion layer is much lower than the conductivity of the p-type neutral layer so that an incremental voltage applied to the pn-junction diode drops predominantly across the depletion layer, rather than the p-type neutral layer. However, if electrons and holes have strongly different mobilities, e.g.,  $\mu_n > 10 \mu_p$ , the above condition is insufficient. In case of a large disparity between electron and hole mobility, the low injection condition needs to be generalized<sup>2</sup>

$$\Delta n_p(0) \mu_n \ll p_{p0} \mu_p. \quad (2)$$

Equation (2), which is more stringent than Eq. (1), illustrates that high-level injection can be more easily reached in pn-junction diodes made of semiconductors with a strong asymmetry in electron and hole mobility ( $\mu_n \gg \mu_p$ ). Semiconductors with such strong asymmetry, which also exhibit the efficiency droop, include GaN (Refs. 3 and 4) (exhibiting droop at 300 K) as well as AlGaInP (Ref. 5) (exhibiting droop at cryogenic temperatures). It was shown that the onset of the efficiency droop in GaInN light-emitting diodes (LEDs) indeed occurs in the high-level injection regime.<sup>2</sup>

Next, we consider the transition from low-level to high-level injection. If the resistance of the depletion region equals that of p-type neutral region, an incremental applied

voltage will drop in equal parts across these regions and the diode has entered the high-level-injection regime. For an n<sup>+</sup>p diode, this can be modeled by a varistor  $R_{\text{Depletion}}$  in series with a resistor  $R_{\text{p-Layer}}$ , representing the depletion-layer and p-type layer, respectively. The p-type layer resistance is given by  $R_{\text{p-Layer}} = L_{\text{p-Layer}} / (e \mu_p p_{p0} A)$ , where  $L_{\text{p-Layer}}$ ,  $e$ , and  $A$  are the p-type layer thickness, the elementary charge, and the junction area, respectively. The depletion-layer resistance is approximately given by  $R_{\text{Depletion}} \approx W_{\text{Depletion}} / (2e \Delta n_p(0) \mu_n A)$ ; (in fact, this is an upper limit). Equating the two resistances yields a condition for the onset of high injection,

$$\Delta n_p(0) \mu_n \approx \frac{W_{\text{Depletion}}}{2L_{\text{p-Layer}}} p_{p0} \mu_p. \quad (3)$$

Considering the geometric factors in the equation, we estimate the onset of high injection to occur when  $\Delta n_p(0) \mu_n$  is about 1% to 10% of  $p_{p0} \mu_p$ .

The internal quantum efficiency (IQE) of an LED can be expressed as the product of the radiative efficiency (RE) in the active region and the injection efficiency (IE), that is,  $\text{IQE} = \text{RE} \times \text{IE}$ . The injection efficiency can be limited by non-capture of carriers into the active region as well as leakage of carriers out of the active region.

In pn heterojunctions, the electron concentration injected into the p-type neutral region is, due to a heterojunction barrier, much smaller than in pn homojunctions. In pn heterojunctions, we denote the electron concentration injected into the p-type neutral region by  $\Delta n_p(0)$ . Given that, in a GaInN LED, the thickness of p-type GaN cladding layer is smaller than the electron diffusion length, we write the electron diffusion current leaking out of the active region of a heterojunction LED as<sup>6</sup>

$$J_{\text{Diffusion}} = \frac{e D_n \Delta n_p(0)}{L_{\text{p-Layer}}}, \quad (4)$$

<sup>a)</sup>Electronic mail: EFSchubert@rpi.edu.

where  $L_{p\text{-Layer}}$  is the thickness of the p-type layer (e.g., the p-type GaN layer),  $e$  is the elementary charge, and  $D_n$  is the electron diffusion coefficient in the p-type layer. As the diode enters high-level injection, some of the applied voltage starts to drop across the low-conductivity p-type layer and a drift current arises. The drift current of electrons injected into the p-type neutral layer, at the edge of the neutral layer, is given by<sup>6</sup>

$$J_{\text{Drift}} = e\mu_n \Delta n_p(0)E = eD_n \frac{e}{kT} \Delta n_p(0) \frac{J_{\text{Total}}}{\sigma_p}, \quad (5)$$

where we employed the Einstein relation, and  $E$ ,  $J_{\text{Total}}$ , and  $\sigma_p$ , are the electric field in the p-type layer, the total current density of the diode, and the p-type layer conductivity ( $\sigma_p = e p_{p0} \mu_p$ ), respectively. The drift-induced leakage current increases with the total current, and will, at a sufficiently large current, become significant. As a consequence, the injection efficiency into the active region is reduced and the device enters the droop regime. It was shown that the onset of the efficiency droop in GaInN LEDs indeed occurs in the high-level injection regime, where an electric field emerges in the p-type GaN layer.<sup>2</sup>

Based on Eq. (4), the leakage current due to electron diffusion is proportional to  $\Delta n_p(0)$ . Assuming purely thermal excitation,  $\Delta n_p(0)$  depends on the carrier concentration in a quantum-well (QW) active region,  $n_{\text{QW}}$ , according to  $\Delta n_p(0) = n_{\text{QW}} \exp(-\Delta E_{\text{Barrier}}/kT)$ ,<sup>6</sup> where  $\Delta E_{\text{Barrier}}$  is the effective energy difference between carriers in the QW and carriers injected into the p-type layer. Several factors can cause the concentration of carriers leaking out of the active region to be higher than expected. *First*, electrons have a carrier temperature that exceeds the lattice temperature. This is illustrated in Figure 1, which shows the electroluminescence spectra of a GaInN LED at different lattice temperatures. Inspection of the figure reveals that the carrier temperature, at a lattice temperature of 300 K, is 425 K. Estimating  $\Delta E_{\text{Barrier}} = 300$  meV and using a carrier temperature of 425 K yields  $\delta = \exp(-\Delta E_{\text{Barrier}}/kT) = 3 \times 10^{-4}$ . *Second*, it is well known that experimental tunneling currents through

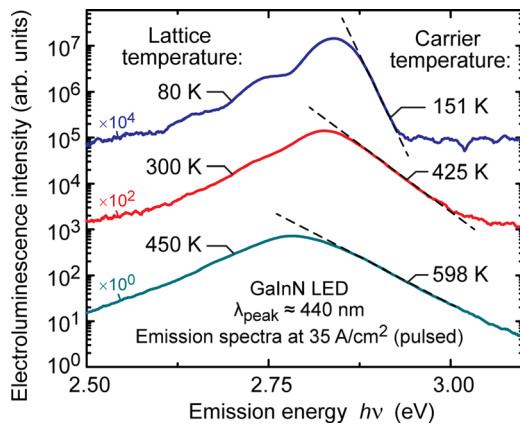


FIG. 1. Emission spectra of a GaInN LED under pulsed injection conditions at different lattice temperatures, showing the carrier temperatures extracted from the high-energy slope of the spectrum using the relation: Intensity  $\propto \exp(-hv/k T_{\text{Carrier}})$ . Under continuous-wave current operation, the carrier temperature will increase further.

barriers are generally higher than theoretical estimates, e.g., by the WKB approximation, due to the participation of defect states located in the barriers.<sup>7</sup> *Third*, polarization fields have been shown to reduce carrier capture and enhance carrier leakage mediated by the positive sheet charge at the spacer-EBL interface in GaInN LEDs.<sup>8</sup> Based on these considerations, we estimate  $\delta$  to be on the order of 0.1%.

The total recombination rate in an LED device has been described by the equation

$$R = A_{\text{SRH}} n_{\text{QW}} + B n_{\text{QW}}^2 + f(n_{\text{QW}}), \quad (6)$$

where  $A_{\text{SRH}}$  is the Shockley-Read-Hall coefficient,  $B$  is the bi-molecular radiative coefficient, and  $f(n_{\text{QW}})$  is a general loss term causing the efficiency droop.<sup>9,10</sup> The loss term,  $f(n_{\text{QW}})$ , includes drift-induced reduction in injection efficiency (drift leakage), as well as Auger recombination. For drift-induced leakage losses,  $f(n)$  will be determined below. For Auger losses,  $f(n) = C_{\text{Auger}} n_{\text{QW}}^3$ , where  $C_{\text{Auger}}$  is Auger coefficient.

Next, we will analyze the carrier-concentration dependence of diffusion- and drift-leakage current densities. The diffusion-leakage current density has the following dependence on carrier concentration:

$$J_{\text{Diffusion}} = \frac{eD_n}{L_{p\text{-layer}}} \Delta n_p(0) = \frac{eD_n}{L_{p\text{-layer}}} \delta n_{\text{QW}}. \quad (7)$$

Close to the peak-efficiency point, where radiative recombination dominates, the recombination rate can be approximated by  $R \approx B n_{\text{QW}}^2$ . In this region, the total current density,  $J_{\text{Total}}$ , depends on the carrier concentration in the QW according to

$$J_{\text{Total}} = e d_{\text{active}} R \approx e d_{\text{active}} B n_{\text{QW}}^2, \quad (8)$$

where  $d_{\text{active}}$  is the active-region thickness. Inserting Eq. (8) into Eq. (5), we find the following dependence of the drift-induced leakage-current density on carrier concentration:

$$J_{\text{Drift}} = e\mu_n \delta n_{\text{QW}} \frac{J_{\text{Total}}}{e\mu_p p_{p0}} \approx e d_{\text{active}} \frac{\delta \mu_n}{\mu_p p_{p0}} B n_{\text{QW}}^3 = e d_{\text{active}} C_{\text{DL}} n_{\text{QW}}^3, \quad (9)$$

where  $C_{\text{DL}}$  is a proportionality constant associated with the lowering of the injection efficiency due to drift of electrons in the p-type layer (“drift leakage”). Since the  $f(n_{\text{QW}}) \propto n_{\text{QW}}^3$  dependence (drift-induced leakage, see Eq. (9)) is stronger than the  $f(n_{\text{QW}}) \propto n_{\text{QW}}$  dependence (diffusion-induced leakage, see Eq. (7)), the latter one may be neglected. Eq. (9) allows one to identify the third-order coefficient as

$$C_{\text{DL}} = \frac{\delta \mu_n}{\mu_p p_{p0}} B. \quad (10)$$

As a numerical example, we choose:  $p_{p0} = 5.0 \times 10^{17} \text{ cm}^{-3}$ ,  $\mu_p = 2.5 \text{ cm}^2/(\text{V s})$ ,  $\mu_n = 300 \text{ cm}^2/(\text{V s})$ ,  $B = 10^{-10} \text{ cm}^3/\text{s}$ , and  $\delta = 0.1\%$ . Using these values, we obtain  $C_{\text{DL}} = 2.4 \times 10^{-29} \text{ cm}^6/\text{s}$ , in agreement with experimental values.<sup>11,12</sup>

At even higher current densities, when the drift-induced leakage current becomes significant, the dependence of the total current density,  $J_{\text{Total}}$ , shifts from a  $J_{\text{Total}} \propto n_{\text{QW}}^2$  dependence to a  $J_{\text{Total}} \propto n_{\text{QW}}^3$  dependence, i.e.,

$$J_{\text{Total}} = ed_{\text{active}}R \approx ed_{\text{active}}C_{\text{DL}}n_{\text{QW}}^3 \quad (11)$$

and consequently, the dominant term of the loss function  $f(n_{\text{QW}})$  shifts from  $f(n_{\text{QW}}) \propto n_{\text{QW}}^3$  to  $f(n_{\text{QW}}) \propto n_{\text{QW}}^4$ . Inserting Eq. (11) into Eq. (9) yields

$$\begin{aligned} J_{\text{Drift}} &= e\mu_n\delta n_{\text{QW}} \frac{J_{\text{Total}}}{e\mu_p p_{p0}} \approx ed_{\text{active}} \left( \frac{\delta\mu_n}{\mu_p p_{p0}} \right)^2 B n_{\text{QW}}^4 \\ &= ed_{\text{active}} D_{\text{DL}} n_{\text{QW}}^4. \end{aligned} \quad (12)$$

The equation allows one to identify the fourth-order coefficient as

$$D_{\text{DL}} = \left( \frac{\delta\mu_n}{\mu_p p_{p0}} \right)^2 B. \quad (13)$$

Therefore, we can write the drift-induced loss term  $f(n_{\text{QW}})$  as:  $f(n_{\text{QW}}) = C_{\text{DL}}n_{\text{QW}}^3 + D_{\text{DL}}n_{\text{QW}}^4 + \dots$ . A fourth-power dependence of  $f(n)$  has indeed been reported in the literature.<sup>13</sup> The total recombination rate can then be written as

$$\begin{aligned} R &= A_{\text{SRH}}n_{\text{QW}} + Bn_{\text{QW}}^2 + f(n_{\text{QW}}) = A_{\text{SRH}}n_{\text{QW}} + Bn_{\text{QW}}^2 \\ &\quad + C_{\text{Auger}}n_{\text{QW}}^3 + C_{\text{DL}}n_{\text{QW}}^3 + D_{\text{DL}}n_{\text{QW}}^4, \end{aligned} \quad (14)$$

where both drift-induced reduction of the injection efficiency as well as Auger losses are included. Squaring Eq. (10) and dividing by Eq. (13) yields

$$C_{\text{DL}}^2 / (D_{\text{DL}}B) = 1.0. \quad (15)$$

This relation between  $B$ ,  $C_{\text{DL}}$ , and  $D_{\text{DL}}$  is helpful in verifying the applicability of the drift-induced-leakage model. To

extract the  $A$ ,  $C$ , and  $D$  coefficients from experiments, the numerical values of the parameters  $d_{\text{active}}$ ,  $B$ , and  $\text{IQE}_{\text{peak}}$  need to be known. However, the extracted ratio  $C^2/(DB)$  does not depend on the numerical values of these parameters.

Next, we present experimental efficiency-versus-current results for three high-quality blue GaInN/GaN LEDs and compare them with the analytic model. The measurements were performed by employment of a Keithley pulse generator using a pulse duration of  $10\ \mu\text{s}$  and a period of 1 ms. The measured external-quantum-efficiency-(EQE)-versus-current-density ( $J$ ) curves of the three LEDs, labeled as LED-N, LED-C, and LED-S, are shown in Figure 2(a). The peak emission wavelength,  $\lambda_{\text{peak}}$ , for LED-N, LED-C, and LED-S is 448 nm, 451 nm, and 448 nm, respectively. In order to plot the total recombination rate,  $R$ , versus  $n_{\text{QW}}$ , we employ a procedure published in a previous report<sup>13</sup> and use a quantum well thickness of  $d_{\text{active}} = 3\ \text{nm}$  and a radiative coefficient of  $B = 1 \times 10^{-10}\ \text{cm}^3/\text{s}$ . The  $R$ -versus- $n_{\text{QW}}$  curve can then be fitted by using the power series  $R = An_{\text{QW}} + Bn_{\text{QW}}^2 + Cn_{\text{QW}}^3 + Dn_{\text{QW}}^4$ . This power series is then converted to an efficiency-versus-current-density curve and an efficiency-versus- $n_{\text{QW}}$  curve, which are shown in Figures 2(a) and 2(b), respectively, along with the numerical values of the  $A$ ,  $B$ ,  $C$ , and  $D$  coefficients. Inspection of the figure reveals: First, the theoretical curves provide an excellent fit to the experimental data. Second, a fit limited to the third power of  $n_{\text{QW}}$  would be insufficient for reaching agreement with experimental data;<sup>13</sup> that is, the experimental EQE<sub>n</sub>-versus- $n_{\text{QW}}$  curve is not symmetric as one would expect based on the ABC model. Third, the values of the  $C$  and  $D$  coefficients obtained from the fit given in Figure 2(a) as well as Eq. (15) reveal a relationship between  $C_{\text{DL}}$  and  $D_{\text{DL}}$ . Therefore, we compare the value of  $C^2/(DB)$  extracted from the fit with the theoretical value of  $C_{\text{DL}}^2/(D_{\text{DL}}B)$  derived from Eq. (15). The extracted ratio  $C^2/(DB)$  for LED-N, LED-C, and LED-S is 0.18, 0.50, and 0.53, respectively, whereas Eq. (15) gives a value of 1.0 for the same ratio. Given that the coefficients  $C$  and  $D$  are

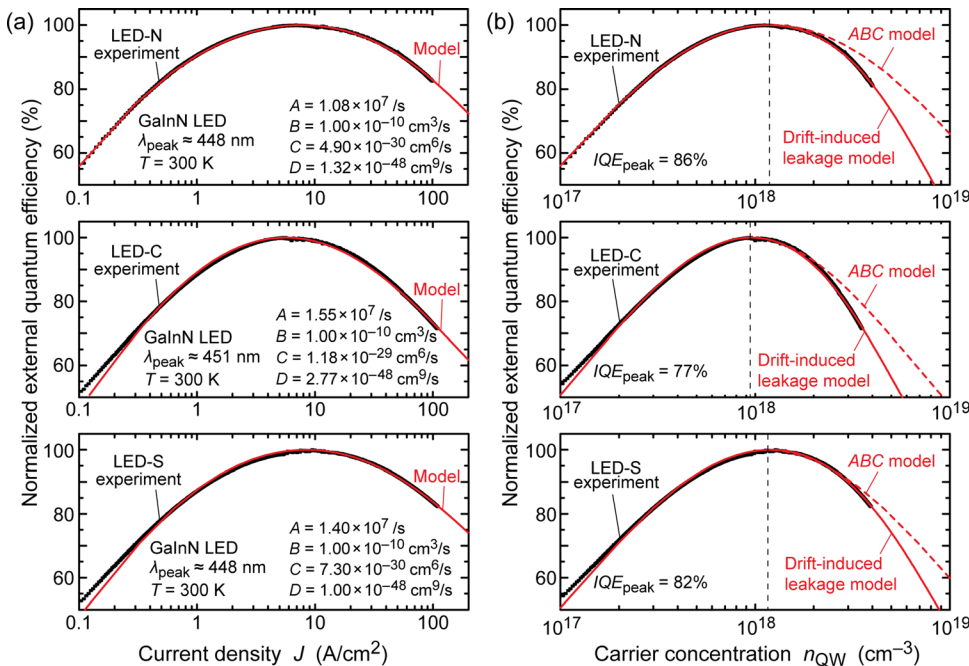


FIG. 2. (a) Room temperature efficiency-versus-injection-current curves for three GaInN LEDs emitting in the blue wavelength range. Also shown are the theoretical fits and the parameters used for the fits based on drift-induced electron leakage. (b) Efficiency-versus-carrier-concentration curves for the three LEDs. Also shown are the theoretical fits. The ABC model shows even symmetry resulting in a discrepancy between experiments and the model at high carrier concentrations. The peak internal quantum efficiency,  $\text{IQE}_{\text{peak}}$ , for LED-N, LED-C, and LED-S is estimated to be 86%, 77%, and 82%, respectively, consistent with the relative peak intensities of the three LEDs.

third- and fourth-order coefficients, we note that the value of the ratio is remarkably close to the theoretical value of 1.0. Besides, the ratio  $(Cn_{\text{QW}}^3)^2/(Bn_{\text{QW}}^2 Dn_{\text{QW}}^4) = C^2/(DB)$  does not depend on the values chosen for  $d_{\text{active}}$ ,  $B$ , and  $\text{IQE}_{\text{peak}}$ .<sup>13</sup>

Finally, based on the analytic model presented here, we calculate the current density at which the efficiency reaches its peak value, i.e., the onset-of-droop current density. Based on the ABC model, the carrier concentration, at which the efficiency reaches its maximum,  $n_{\text{peak-IQE}}$ , can be expressed as<sup>13</sup>

$$n_{\text{peak-IQE}} = \sqrt{A_{\text{SRH}}/C}, \quad (16)$$

where we neglected the contribution of 4th-order terms (i.e., the  $D$  coefficient). Near the peak efficiency, the total recombination rate  $R$  is dominated by  $Bn_{\text{QW}}^2$ . Therefore, based on the drift-induced leakage model, the onset-of-droop current density can be expressed as

$$\begin{aligned} J_{\text{Onset-of-droop}} &= ed_{\text{active}}Bn_{\text{peak-IQE}}^2 = ed_{\text{active}} \frac{BA_{\text{SRH}}}{C_{\text{DL}}} \\ &= ed_{\text{active}}A_{\text{SRH}} \frac{p_{\text{p0}}\mu_{\text{p}}}{\delta\mu_{\text{n}}}. \end{aligned} \quad (17)$$

As a numerical example, we use the parameters  $d_{\text{active}} = 3.0 \text{ nm}$ ,  $A_{\text{SRH}} = 1.0 \times 10^7/\text{s}$ ,  $p_{\text{p0}} = 5.0 \times 10^{17} \text{ cm}^{-3}$ ,  $\mu_{\text{p}} = 2.5 \text{ cm}^2/(\text{V s})$ ,  $\mu_{\text{n}} = 300 \text{ cm}^2/(\text{V s})$ , and  $\delta = 0.1\%$ . Using these values in the above equation, we calculate an onset-of-droop current density of  $2.0 \text{ A/cm}^2$ . This value is within the range of experimental onset-of-droop current densities, which typically are between  $1.0$  and  $10 \text{ A/cm}^2$ .<sup>2,14,15</sup>

In conclusion, an analytic model is developed for the droop in the efficiency-versus-current curve for LEDs made from semiconductors having a strong asymmetry in carrier concentration and mobility. For pn-junction diodes made of such semiconductors, the high-injection condition, which is generalized to include mobilities, can be easily reached. Under high-injection conditions, electron drift in the p-type layer of the diode causes a decrease of the injection efficiency and an associated reduction in internal quantum efficiency. The drift-induced leakage function is shown to have a 3rd-order as well as a 4th-order dependence on

the carrier concentration.  $C_{\text{DL}}$  is found to be approximately  $10^{-29} \text{ cm}^6/\text{s}$ . An analytic formula giving the onset-of-droop current density in LEDs is derived. The analytic model very well explains the experimental efficiency-versus-current curves of GaInN LEDs.

The authors gratefully acknowledge support by Samsung LED Company, Sandia National Laboratories, the US National Science Foundation, the Korean Ministry of Knowledge Economy, the Korea Institute for Advancement of Technology, and Magnolia Optical Technologies, Inc. Authors G.-B.L., D.S.M., J.C., and E.F.S. were supported by Sandia's Solid-State Lighting Sciences Center, an Energy Frontier Research Center funded by the U.S. Department of Energy, Office of Basic Energy Sciences.

<sup>1</sup>W. Shockley, *Electrons and Holes in Semiconductors* (Van Nostrand, Princeton, NJ, 1950).

<sup>2</sup>D. S. Meyaard, G.-B. Lin, Q. Shan, J. Cho, E. F. Schubert, H. Shim, M.-H. Kim, and C. Sone, *Appl. Phys. Lett.* **99**, 241114 (2011).

<sup>3</sup>T. T. Mnatsakanov, M. E. Levinshtein, L. I. Pomortseva, S. N. Yurkov, G. S. Simin, and M. A. Khan, *Solid-State Electron.* **47**, 111 (2003).

<sup>4</sup>P. Kozodoy, H. Xing, S. P. DenBaars, U. K. Mishra, A. Saxler, R. Perrin, S. Elhamri, and W. C. Mitchel, *J. Appl. Phys.* **87**, 1832 (2000).

<sup>5</sup>J.-I. Shim, D.-P. Han, H. Kim, D.-S. Shin, G.-B. Lin, D. S. Meyaard, Q. Shan, J. Cho, E. F. Schubert, H. Shim, and C. Sone, *Appl. Phys. Lett.* **100**, 111106 (2012).

<sup>6</sup>E. F. Schubert, *Light-Emitting Diodes*, 2nd ed. (Cambridge University Press, Cambridge, 2006).

<sup>7</sup>X. A. Cao, E. B. Stokes, P. M. Sandvik, S. F. LeBoeuf, J. Kretschmer, and D. Walker, *IEEE Electron Device Lett.* **23**, 535 (2002).

<sup>8</sup>M.-H. Kim, M. F. Schubert, Q. Dai, J. K. Kim, E. F. Schubert, J. Piprek, and Y. Park, *Appl. Phys. Lett.* **91**, 183507 (2007).

<sup>9</sup>D. S. Meyaard, Q. Shan, Q. Dai, J. Cho, E. F. Schubert, M.-H. Kim, and C. Sone, *Appl. Phys. Lett.* **99**, 041112 (2011).

<sup>10</sup>Q. Dai, Q. Shan, J. Wang, S. Chhajed, J. Cho, E. F. Schubert, M. H. Crawford, D. D. Koleske, M.-H. Kim, and Y. Park, *Appl. Phys. Lett.* **97**, 133507 (2010).

<sup>11</sup>J. Piprek, *Phys. Status Solidi A* **207**, 2217 (2010).

<sup>12</sup>H.-Y. Ryu, H.-S. Kim, and J.-I. Shim, *Appl. Phys. Lett.* **95**, 081114 (2009).

<sup>13</sup>Q. Dai, Q. Shan, J. Cho, E. F. Schubert, M. H. Crawford, D. D. Koleske, M.-H. Kim, and Y. Park, *Appl. Phys. Lett.* **98**, 033506 (2011).

<sup>14</sup>M. F. Schubert, J. Xu, J. K. Kim, E. F. Schubert, M. H. Kim, S. Yoon, S. M. Lee, C. Sone, T. Sakong, and Y. Park, *Appl. Phys. Lett.* **93**, 041102 (2008).

<sup>15</sup>Y.-L. Li, Y.-R. Huang, and Y.-H. Lai, *Appl. Phys. Lett.* **91**, 181113 (2007).